Supplement of Earth Syst. Sci. Data, 10, 1591–1603, 2018
https://doi.org/10.5194/essd-10-1591-2018-supplement

Supplement of

Estimating the thickness of unconsolidated coastal aquifers along the global coastline

D. Zamrsky et al.

Correspondence to: Daniel Zamrsky (d.zamrsky@uu.nl)

Table S1. Borehole validation dataset sources

Dataset Name	Source
CPRM	Geological survey of Brazil, c2016, published by Companhia de Pesquisa de Recursos Minerais [Accessed 2016, August], http://www.cprm.gov.br/
GeoVIC	Online geology portal of Victoria, Australia, c2016, published by the state of Victoria [Accessed 2016, October], http://er-info.dpi.vic.gov.au/sd_weave/anonymous.html
CGS	China Geological Survey, 2012. Groundwater serial maps of Asia: Hydrogeological map, Groundwater resources map, Geothermal map, Sinomaps Press.

Table S2. Literature validation dataset sources

Polygon ID	Source
1	Lagudu, S. et al., 2013. Use of Geophysical and Hydrochemical Tools to Investigate Seawater Intrusion in Coastal Alluvial Aquifer, Andhra Pradesh, India. In C. Wetzelhuetter, ed. Groundwater in the Coastal Zones of Asia-Pacific. Dordrecht: Springer Netherlands, pp. 49–65.
2	Singh, S.C., 2013. Geophysical Viewpoints for Groundwater Resource Development and Management in Coastal Tracts. In C. Wetzelhuetter, ed. Groundwater in the Coastal Zones of Asia-Pacific. Dordrecht: Springer Netherlands, pp. 67–87.
3	Duerrast, H. & Srattakal, J., 2013. Geophysical Investigations of Saltwater Intrusion into the Coastal Groundwater Aquifers of Songkhla City, Southern Thailand. In C. Wetzelhuetter, ed. Groundwater in the Coastal Zones of Asia-Pacific. Dordrecht: Springer Netherlands, pp. 155–175.
4	Sherif, M., Almulla, M. & Shetty, A., 2013. Seawater Intrusion Assessment and Mitigation in the Coastal Aquifer of Wadi Ham. In C. Wetzelhuetter, ed. Groundwater in the Coastal Zones of Asia-Pacific. Dordrecht: Springer Netherlands, pp. 271–294.
5	Leonhard, L., Burton, K. & Milligan, N., 2013. Gascoyne River, Western Australia; Alluvial Aquifer, Groundwater Management and Tools. In C. Wetzelhuetter, ed. Groundwater in the Coastal Zones of Asia-Pacific. Dordrecht: Springer Netherlands, pp. 359–378.
6	Wagner, F., Tran, V.B. & Renaud, F.G., 2012. Groundwater Resources in the Mekong Delta: Availability, Utilization and Risks. In F. G. Renaud & C. Kuenzer, eds. The Mekong Delta System: Interdisciplinary Analyses of a River Delta. Dordrecht: Springer Netherlands, pp. 201–220.
7	Benkabbour, B., Toto, E.A. & Fakir, Y., 2004. Using DC resistivity method to characterize the geometry and the salinity of the Plioquaternary consolidated coastal

	aquifer of the Mamora plain, Morocco. Environmental Geology, 45(4), pp.518–526. Available at: http://link.springer.com/10.1007/s00254-003-0906-y. Amharref, M. et al., 2007. Cartographie de la vulnérabilité à la pollution des eaux souterraines: Application à la plaine du Gharb (Maroc). Journal of Water Science, 20(2), pp.185–199.
8	Chen, J. et al., 2014. Clay minerals in the Pliocene - Quaternary sediments of the southern Yangtze coast, China: Sediment sources and palaeoclimate implications. Journal of Palaeogeography, 3(3), pp.297–308. Available at: http://dx.doi.org/10.3724/SP.J.1261.2014.00057.
9	Cobaner, M. et al., 2012. Three-dimensional simulation of seawater intrusion in coastal aquifers: A case study in the Goksu Deltaic Plain. Journal of Hydrology, 464-465, pp.262–280. Available at: http://dx.doi.org/10.1016/j.jhydrol.2012.07.022.
10	Carretero, S. et al., 2013. Impact of sea-level rise on saltwater intrusion length into the coastal aquifer, Partido de La Costa, Argentina. Continental Shelf Research, 61-62, pp.62–70. Available at: http://dx.doi.org/10.1016/j.csr.2013.04.029.
11	Rasmussen, P. et al., 2013. Assessing impacts of climate change, sea level rise, and drainage canals on saltwater intrusion to coastal aquifer. Hydrology and Earth System Sciences, 17(1), pp.421–443. Available at: http://www.hydrol-earth-syst-sci.net/17/421/2013/.
12	Kalm, V. & Gorlach, A., 2014. Impact of bedrock surface topography on spatial distribution of Quaternary sediments and on the flow pattern of late Weichselian glaciers on the East European Craton (Russian Plain). Geomorphology, 207, pp.1–9. Available at: http://dx.doi.org/10.1016/j.geomorph.2013.10.022.
13	Chen, J. et al., 2014. Clay minerals in the Pliocene - Quaternary sediments of the southern Yangtze coast, China: Sediment sources and palaeoclimate implications. Journal of Palaeogeography, 3(3), pp.297–308. Available at: http://dx.doi.org/10.3724/SP.J.1261.2014.00057.
14	Sefelnasr, A. & Sherif, M., 2014. Impacts of Seawater Rise on Seawater Intrusion in the Nile Delta Aquifer, Egypt., 52(2), pp.264–276.
15	Singaraja, C. et al., 2015. A study on the status of saltwater intrusion in the coastal hard rock aquifer of South India. Environment, Development and Sustainability, 17(3), pp.443–475. Available at: http://dx.doi.org/10.1007/s10668-014-9554-5.
16	Khaki, M. et al., 2016. Integrated geoelectrical and hydrogeochemical investigation for mapping the aquifer at Langat Basin, Malaysia. Environmental Earth Sciences, 75(4), pp.1–14. Available at: "http://dx.doi.org/10.1007/s12665-015-5182-0.
17	Giresse, P. et al., 2000. Successions of sea-level changes during the Pleistocene in Mauritania and Senegal distinguished by sedimentary facies study and U / Th dating., 170. Sylla, M., Medou, J.O. & Samb, E.., 1997. Contribution of the instaneous well logging to the study of the indurations. Bulletin of the International Association of Engineering Geology, (55).
18	Nicholas, C.J. et al., 2006. Stratigraphy and sedimentology of the Upper Cretaceous to Paleogene Kilwa Group, southern coastal Tanzania. , 45, pp.431–466.
19	Y. Yechieli, O. Sivan (2010), Using geochemical tools to study the distribution of saline groundwater in aquifers separated by aquitards: examples from Israel, paper presented at the 21th Salt Water Intrusion Meeting, Azores, Portugal
20	Dirks et al. (1988), Groundwater in Bekasi district, West Java, Indonesia, paper presented at the 10th Salt Water Intrusion Meeting, Gent, Belgium
21	McPherson, A. & Jones, A., 2005. Appendix D: Perth Basin geology review and site class assessment. Natural Hazard Risk in Perth, pp.313–344. Available at: https://www.icsm.gov.au/image_cache/GA6548.pdf.
22	Ransley, T.R., Radke, B.M., Feitz, A.J., Kellett, J.R., Owens, R., Bell, J., Stewart, G. and Carey, H. 2015. Hydrogeological Atlas of the Great Artesian Basin, Geoscience Australia, Canberra.

	http://dx.doi.org/10.11636/9781925124668
23	Yeates, A.N. et al., 1984. Regional geology of the onshore Canning Basin, Western Australia. The Canning Basin, Western Australia, pp.23–56.
24	E. Custodio (1992), Preliminary outlook of saltwater intrusion conditions in the Donana National Park (southern Spain), paper presented at 12th Salt Water Intrusion Meeting, Barcelona, Spain J.L. Plata and F.M. Rubio (2004), Study of the salt water - fresh water interface in environments of low resistivity: Donana aquifer (Spain), paper presented at the 18th Salt Water Intrusion Meeting, Cartagena, Spain
25	Custodio, E., V. Iribar, M. Manzano, A. Bayó and A. Galofré (1986), Evolution of sea water intrusion in the Llobregat Delta, Barcelona, Spain, paper presented at the 9th Salt Water Intrusion Meeting, Delft, The Netherlands E. Falgas, J. Ledo, T. Teixido, A. Gabas, F. Ribera, C. Arango, P. Queralt, J.L. Plata, F.M. Rubio, J.A. Pena, A. Marti, A. Marcuello (2004), Geophysical characterization of a mediterranean coastal aquifer: The Baixa Tordera fluvio-deltaic aquifer unit (Barcelona, NE Spain), paper presented at the 18th Salt Water Intrusion Meeting, Cartagena, Spain
26	B. Aunay, C. Duvail, P. Le Strat, N. Dorfliger, P. Lachassagne and S. Pistre (2004), Importance of a high resolution lithological and geometrical knowledge for Mediterranean coastal sedimentary aquifers management. Application to the Roussillon basin, South of France, paper presented at the 18th Salt Water Intrusion Meeting, Cartagena, Spain
27	P. Cau, G. Lecca, L. Muscas, G. Barrocu and G. Uras (2002), Seawater intrusion in the plain of Oristano (Sardinia, Italy), paper presented at the 17th Salt Water Intrusion Meeting, Delft, The Netherlands
28	F. Ardau, R. Balia, G. Barbieri, G. Barrocu, E. Gavaudo and G. Ghiglieri (2002), Recent development in hydrogeological and geophysical research in the Muravera coastal plain (SE Sardinia, Italy), paper presented at the 17th Salt Water Intrusion Meeting, Delft, The Netherlands
29	V. Ferrara and A. Pennisi (2004), Salt water intrusion and its influence on groundwater use in the Siracusa area (south-eastern Sicily), paper presented at the 13th Salt Water Intrusion Meeting, Cagliari, Italy
30	A. Bencini & G. Pranzini (1992), The salinization of groundwaters in the Grosseto Plain (Tuscany, Italy), paper presented at the 12th Salt Water Intrusion Meeting, Barcelona, Spain
31	G. Pranzini (2002), Groundwater salinization in Versilia (Italy), paper presented at the 17th Salt Water Intrusion Meeting, Delft, The Netherlands
32	E. Van Houtte, L. Lebbe, L. Zeuwts and F. Vanlerberghe (2002), Concept for development of sustainable drinking-water production in the Flemish coastal plain based on integrated water management, paper presented at the 17th Salt Water Intrusion Meeting, Delft, The Netherlands Lebbe, L.C. and K. Pede (1986), Salt-fresh water flow underneath old dunes and low polders influenced by pumpage and drainage in the Western Belgian coastal plain, paper presented at 9th Salt Water Intrusion Meeting, Delft, The Netherlands Lebbe, L. and K. Walraevens (1988), Hydrogeological SWIM-excursion to the western coastal plain of Belgium, paper presented at the 10th Salt Water Intrusion Meeting, Gent, Belgium
33	Lotringen, I.G.J, van, and R. H. Boekelman (1986), Behaviour of circular fresh water lenses, paper presented at the 9th Salt Water Intrusion Meeting, Delft, The Netherlands Meerten, J.J. van, and R.H. Boekelman (1986), Well-infiltration in fresh-water pockets in sandy ridges in Zeeland, paper presented at the 9th Salt Water Intrusion Meeting, Delft, The Netherlands Walraevens et al. (1988), Hydrogeological SWIM-excursion to the Black-Sluice Polder

	area in the Flemish Valley of Belgium, paper presented at the 10th Salt Water Intrusion Meeting, Gent, Belgium
34	Delsman, J.R. et al., 2013. Palaeo-modeling of coastal salt water intrusion during the Holocene: an application to the Netherlands. Hydrology and Earth System Sciences Discussions, 10(11), pp.13707–13742. Available at: http://www.hydrol-earth-syst-sci-discuss.net/10/13707/2013/hessd-10-13707-2013.html. G.H.P. Oude Essink (2002), Salinization of the Wieringermeerpolder, The Netherlands, paper presented at the 17th Salt Water Intrusion Meeting, Delft, The Netherlands P.J. Stuyfzand (1992), Behaviour of major and trace consituents in fresh and salt intrusion waters, in the western Netherlands, paper presented at the 12th Salt Water Intrusion Meeting, Barcelona, Spain Stuyfzand, P.J. (1988), Hydrochemical evidence of fresh- and salt-water intrusions in the coastal dunes aquifer system of the western Netherlands, paper presented at the 10th Salt Water Intrusion Meeting, Gent, Belgium Pomper, A.B. (1972), Evidence of the influence of man on the natural processes related with salinization of groundwater in the western part of West-Netherlands, paper presented at the 3rd Salt Water Intrusion Meeting, Copenhagen, Denmark Roebert, A.J. (1972), Salt water contamination of the wells along the Barnaart-Schuster Canal in the Amsterdam Dune Water Catchment Area, paper presented at the 3rd Salt Water Intrusion Meeting, Copenhagen, Denmark Roebert, A.J. (1972), Salt water contamination of the wells along the Barnaart-Schuster Canal in the Amsterdam Dune Water Catchment Area, paper presented at the 3rd Salt Water Intrusion Meeting, Copenhagen, Denmark Pomper, A.B. (1977), An estimation of chloride intrusion in the midwest Netherlands during the Pleistocene epoch, paper presented at the 5th Salt Water Intrusion Meeting, Medmenham, United Kingdom De Vries, J.J. (1981), The distribution of fresh and salt groundwater in the Dutch coastal area and the Quaternary-geological evolution, paper presented at the 7th Salt Water Intrusion Meeting, Uppsala, Sweden
35	A. Rogge & V. Josopait (1992), Salinization caused by groundwater abstraction from an aquifer on the german North Sea coast, paper presented at the 12th Salt Water Intrusion Meeting, Barcelona, Spain
36	M.D. Fidelibus, E. Gimenez, I. Morell & L. Tulipano (1992), Salinization processes in the Castellon plain aquifer (Spain), paper presented at the 12th Salt Water Intrusion Meeting, Barcelona, Spain
37	A. Bayo, C. Loaso, J.M. Aragones & E. Custodio (1992), Marine intrusion and brackish water in coastal aquifers of Southern Catalonia and Castello (Spain): a brief survey of actual problems and circumstances, paper presented at the 12th Salt Water Intrusion Meeting, Barcelona, Spain
38	M. Fidelibus, F. Caporale and G. Spilotro (2004), Studies on different kinds of salinisation in the ground waters of the Ionian coastal plain of the Basilicata region, paper presented at the 18th Salt Water Intrusion Meeting, Cartagena, Spain
39	(Planert & Williams 1995)
40, 41	Olcott, P.G., 1995. Ground Water Atlas of the United States: Segment 12, Connecticut, Maine, Massachusetts, New Hampshire, New York, Rhode Island, Vermont - ed., Available at: http://pubs.er.usgs.gov/publication/ha730M.
42, 43, 44	Trapp Jr., H. & Horn, M.A., 1997. Ground Water Atlas of the United States: Segment 11, Delaware, Maryland, New Jersey, North Carolina, Pennsylvania, Virginia, West Virginia - ed.,
45	Ryder, P.D., 1996. Ground Water Atlas of the United States: Segment 4, Oklahoma, Texas - ed., Available at: http://pubs.er.usgs.gov/publication/ha730E.
46, 47, 48	Renken, R.A., 1998. Ground Water Atlas of the United States: Segment 5, Arkansas, Louisiana, Mississippi - ed.,
49, 50, 51	Whitehead, R.L., 1994. Ground Water Atlas of the United States: Segment 7, Idaho,

	Oregon, Washington - ed.,
52, 53, 54	Planert, M. & Williams, J.S., 1995. Ground Water Atlas of the United States: Segment 1, California, Nevada - ed.,
55, 56, 57, 58, 59	Miller, J.A., 1990. Ground Water Atlas of the United States: Segment 6, Alabama, Florida, Georgia, South Carolina - ed., Available at: http://pubs.er.usgs.gov/publication/ha730G.
60	Tuttle, M.L.W., Charpentier, R. & Brownfield, M.E., 1999. The Niger Delta Petroleum System: Niger Delta Province, Nigeria, Cameroon, and Equatorial Guinea, Africa. World Energy Project, (99-50-H), p.64.
61	M. Gennessaux, P.B. and E.W., 1998. Thickness of the Plio-Quaternary sediments (IBCM-PQ). BOLLETTINO DI GEOFISICA TEORICA ED APPLICATA, 39(4), pp.243–284.
62	Al Farrah, N., Van Camp, M. & Walraevens, K., 2013. Deducing transmissivity from specific capacity in the heterogeneous upper aquifer system of Jifarah Plain, NW-Libya. Journal of African Earth Sciences, 85, pp.12–21. Available at: http://dx.doi.org/10.1016/j.jafrearsci.2013.04.004.
63	Van Camp, M. et al., 2014. Investigating seawater intrusion due to groundwater pumping with schematic model simulations: The example of the Dar es Salaam coastal aquifer in Tanzania. Journal of African Earth Sciences, 96, pp.71–78. Available at: http://dx.doi.org/10.1016/j.jafrearsci.2014.02.012.
64	Kumar, B. et al., 2011. Groundwater management in a coastal aquifer in Krishna River Delta, South India using isotopic approach. , 100(7).

Table S3. Aquifer thickness information provided by the literature sources compared with the ATE values for each coastal area (column “id”, corresponds to ID values in Figure S6). For each are the location is also given. The values from literature are shown in columns below the “Measured values” header while our ATE values are below the “ATE values” header. The “calc_avg” column represents the calculated average value in cases where only min., max. or both were given by the literature. The “calc_avg” is calculated as either the arithmetic average between the min. and max. values or as min./max. value +/- half of min./max.

	Measured values (m)				ATE values (m)			
id	**thick_max**	**thick_min**	**thick_avg**	**calc_avg**	**est_avg**	**est_min**	**est_max**	**location**
1	600			300	501.1	323.1	768.0	Godavari delta (IND)
2			130	130	174.8	76.2	386.9	Digha (IND)
3			80	80	76.2	35.7	173.9	Songkhla (THA)
4			100	100	84.6	36.0	124.1	Wadi Ham (UAE)
5			50	50	72.9	41.2	120.0	Carnavon (AUS)
6	600			300	272.2	51.0	897.8	Mekong (VNM)
7	100	20	70	70	116.9	30.6	244.3	Rabat (MAR)
8	500	300		400	281.0	41.7	648.4	South Jangtze coast, NE (CHN)
9	600			300	161.9	64.9	308.4	Goksu plain (TUR)
10	20			10	34.9	22.3	51.2	Mar de Ajo (ARG)
11			50	50	277.4	49.0	750.8	Falster island (DKN)
12			50	50	215.6	2.1	5143.4	Riga gulf (EST)
13			200	200	238.5	53.5	615.2	South Jangtze coast, SW (CHN)
14	900			450	484.8	33.5	1394.4	Nile delta (EGY)
15	45		25	25	210.1	83.8	333.9	Thamirabarani delta (IND)
16	100			50	190.9	93.5	310.7	Kuala Lumpur (MYS)
17	150			75	79.9	2.2	371.3	Saloum delta (SEN)
18		1000			261.0	40.7	984.0	Kilwa group (TZA)
19	250		200	200	278.9	44.8	649.5	Coastal aquifer (ISR)
20	300		250	250	268.8	41.5	483.1	Bekasi (IDN)
21	420			210	110.9	9.4	331.7	Perth Basin (AUS)
22	1000	50	600	600	161.8	5.0	1091.9	Great artesian basin (AUS)
23	120			60	106.8	1.1	496.4	Canning Basin (AUS)
24	1000	150		575	166.0	53.4	399.6	Doñana National Park (ESP)
25	180	50		115	109.7	67.3	186.5	Barcelona (ESP)
26	200	80		140	119.0	39.8	163.9	Perpignan (FRA)
27	218	18	120	120	104.2	0.4	247.3	Oristano (ITA)
28	300			150	84.1	40.7	128.5	Muravera (ITA)
29	100			50	177.6	89.2	236.5	Siracusa (ITA)
30	200			100	150.8	81.1	201.2	Grosseto (ITA)
31		100		200	153.4	2.1	317.0	Versilia (ITA)
32	150	25	100	100	116.8	54.5	312.9	Coastal aquifer (BEL)
33	315	30	90	90	185.2	62.1	436.4	Northern dutch coast (NLD)
34	600	100	200	200	441.1	165.4	875.9	Zeeland (NLD)
35	175	125		150	66.3	16.6	261.9	Wilhelmshaven (GER)
36	200	80		140	125.7	58.4	180.0	Castellon de la Plana (ESP)
37			200	200	187.8	91.5	429.0	Ebro delta (ESP)
38			100	100	131.6	78.8	211.3	Scanzano (ITA)
39	300			150	123.7	13.5	331.6	Eureka aquifer, CA (USA)
40	300	30		165	165.8	28.3	520.4	Cape Cod (USA)
41	600	170		385	260.8	1.4	1245.4	Long Island (USA)
42	1200			600	285.0	33.7	815.5	North Atlantic coastal plain, NJ (USA)
43	2400			1200	295.9	21.8	2028.6	North Atlantic coastal plain, MA (USA)
44	3100			1550	444.8	6.4	4983.9	North Atlantic coastal plain, NC (USA)
45	2000	300		1150	266.5	24.5	2652.5	Coastal lowlands aq. system, TX (USA)
46	2400	1200		1800	83.9	72.9	94.8	Coastal lowlands aq. system SE, LA (USA)
47	3600	1200		2400	367.7	120.6	1085.5	Coastal lowlands aq. system NW, LA (USA)
48	1000			500	204.7	22.2	815.7	Mississippi emayment aq. (USA)
49	1000			500	130.8	2.2	496.7	Puget-Williamette trough regional aq. system (USA)
50	35	15		25	97.4	16.2	388.0	Washington coast N (USA)
51	200	35		117.5	138.7	14.1	318.1	Washington coast S (USA)
52	300			150	75.7	3.7	182.3	Santa Clara valley (USA)
53	300			150	162.9	92.7	204.2	Salinas Valley (USA)
54	1200	30		615	286.6	130.3	492.4	Los Angeles - Orange county (USA)
55	1000	200		600	170.2	7.0	1762.3	FL - W and AL coast (USA)
56	1050	850		950	95.5	1.9	1172.4	FL - S (USA)
57	200	60		130	210.7	30.0	1293.4	SC - S (USA)
58	850	200		525	167.0	52.0	723.7	Georgia coast (USA)
59	850	700		775	189.5	6.1	2079.0	FL - N (USA)
60	2000			1000	171.7	1.3	805.5	Niger delta (NGA)
61	1200			600	415.4	46.3	929.4	Po delta (ITA)
62	180	30		105	247.3	4.7	490.5	Jifarah Plain (LBY)
63			150	150	295.2	88.0	1049.5	Dar es Salaam (TZA)
64	450	40		245	286.6	65.2	608.0	Kirishna river delta (IND)

Table S4 Parameter values for the three cross-sections, the values are given for models with minimum and maximum estimated sediment thickness at the coastline. The total length of simulation for the test case in Virginia, USA is larger than for the other two test cases due to the complexity and size of the aquifer system. This was done to ensure that the steady-state (or near steady-state) is reached, for the changes of fresh groundwater cells in time see Figure S10 in the Supplementary information.

	Italy		Israel		Virginia, USA	
Sediment thickness at coastline	50m	500m	100m	1400m	200m	1500m
Number of columns	1,060	1,588	385	494	547	578
Number of layers	53	411	43	110	44	106
Layer thickness (m)	3		10		10	
Column width (m)	25		100		500	
Top elevation (m asl.)	26		95		59	
Bottom elevation (m asl.)	-62	-1,002	-335	-1,005	-381	-1,001
Length of simulation (years)	10,000				100,000	
Number of time steps	2,500				10,000	
Total active cells	13,224	534,879	3,021	30,332	9,319	43,630
Horizontal hydraulic conductivity aquifer (m/d)	10					
Vertical hydraulic conductivity aquifer (m/d)	1					
Horizontal hydraulic conductivity aquitard (m/d)	1.00E-04		1.00E-04		1.00E-04	
Vertical hydraulic conductivity aquitard (m/d)	1.00E-07		1.00E-07		1.00E-07	
Layer type	confined					
Total amount of GHB cells	887	1415	200	321	274	431
Recharge rate (m/d)	0.001		0.0005			
Head change criterion for convergence (m)	1.00E-04					
Residual criterion for convergence (m^3/d)	10					
Porosity	0.35					
Solver type	Finite Difference					
Longitudinal dispersivity	1					
Ratio horizontal transverse disp./ long. disp.	0.1					
Diffusion coefficient (m^2/d)	8.64E-05					

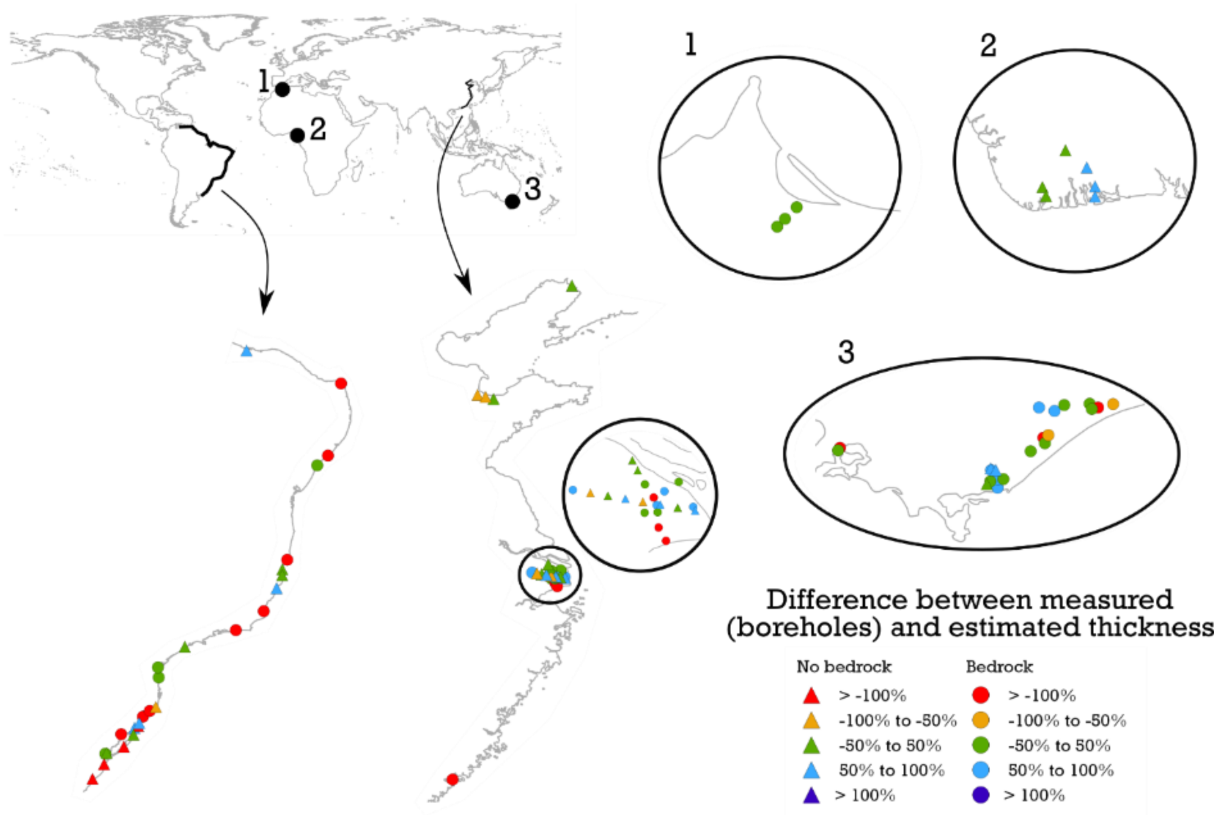

Figure S1. Schematization of borehole validation using the difference between the measured sediment thickness and an average estimated thickness in a radius of 2.5km around the borehole location. The boreholes are divided into two groups depending on any bedrock formation indicated in the borehole report.

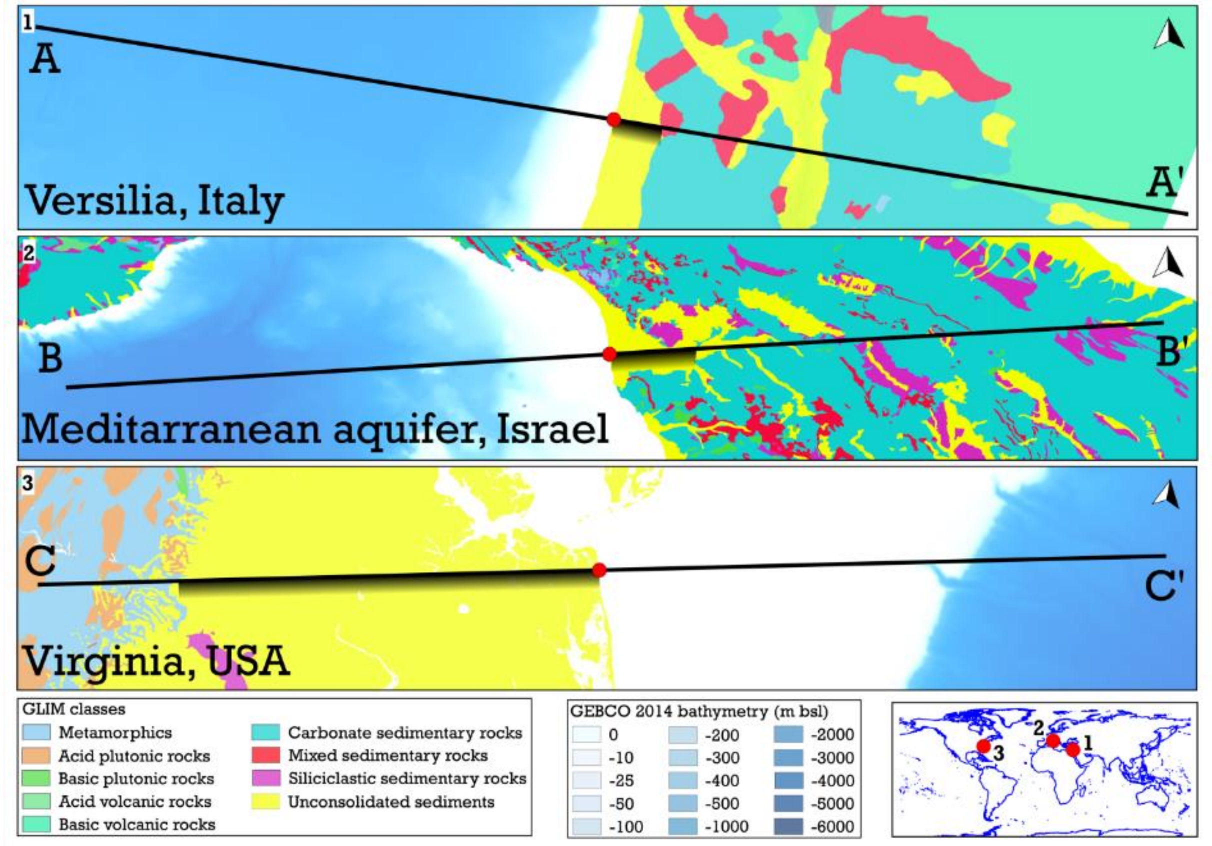

Figure S2. Location of the cross-sections used as examples to illustrate the ATE method. The black shadow represents the extent of the coastal plain in each cross-section while the whole black line indicates the span of the cross-section (in total 400km).

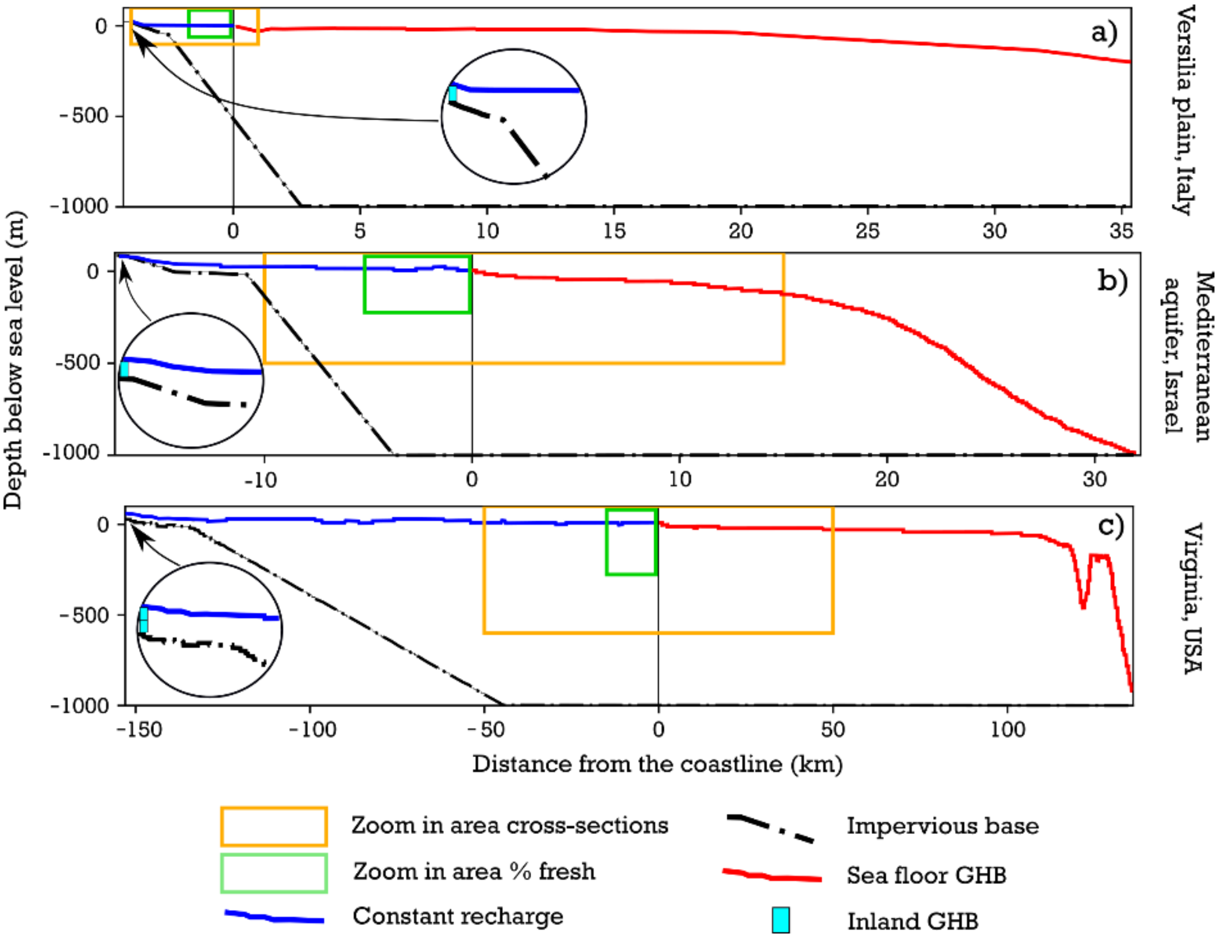

Figure S3. Model concept schematization for all three test cases. a) Versilia plain, Italy, b) Mediterranean aquifer, Israel and c) Virginia, USA. The zoom in area cross-section corresponds to the areas shown in Figures S8-S10 and Figure 4 in the main article.

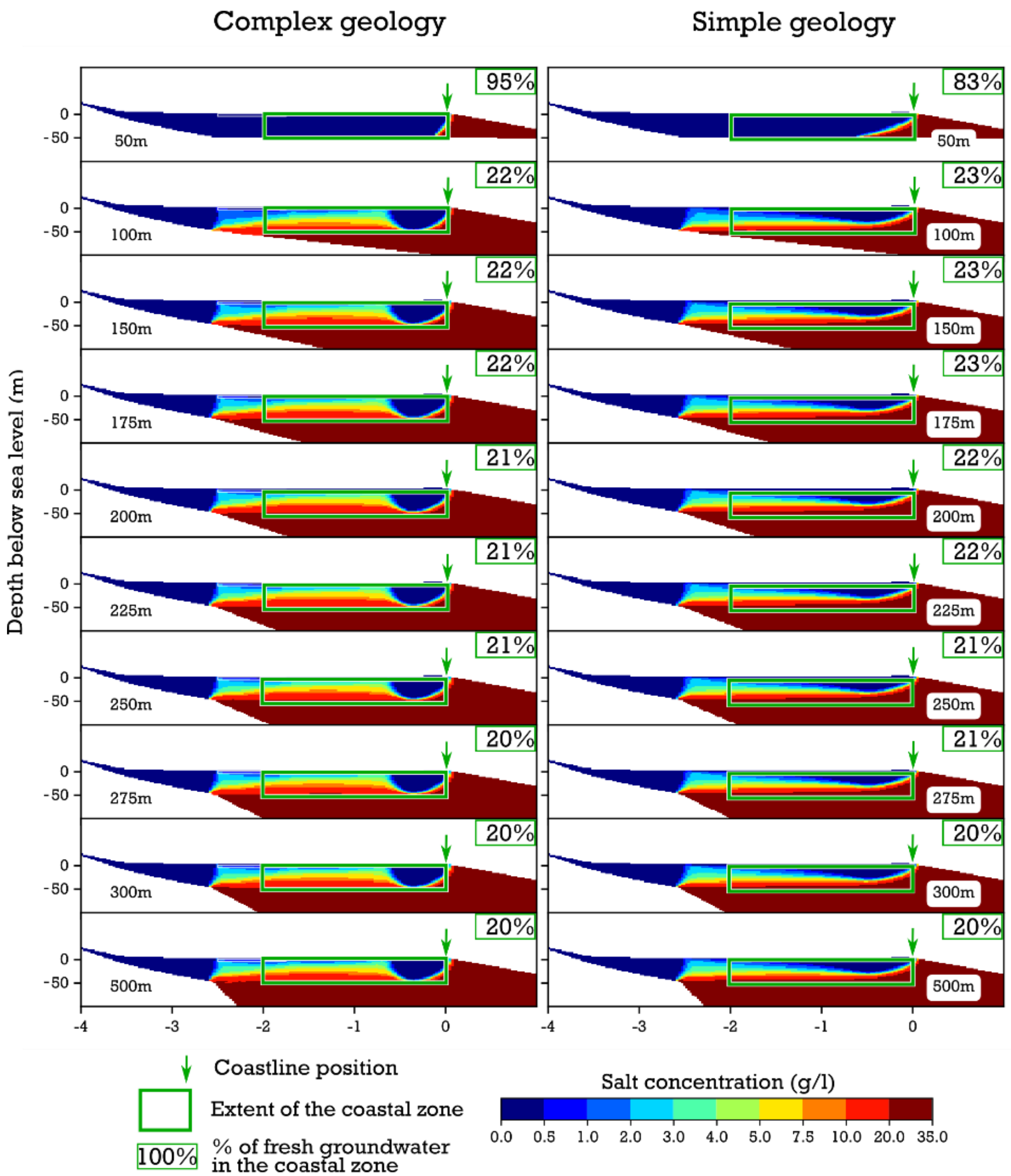

Figure S4. Simulation results for the cross-section located in Versilia plain, Italy. Salt concentration profiles are given for various sediment thicknesses at the coastline and two different geological scenarios (homogeneous and heterogeneous based on information provided by literature).

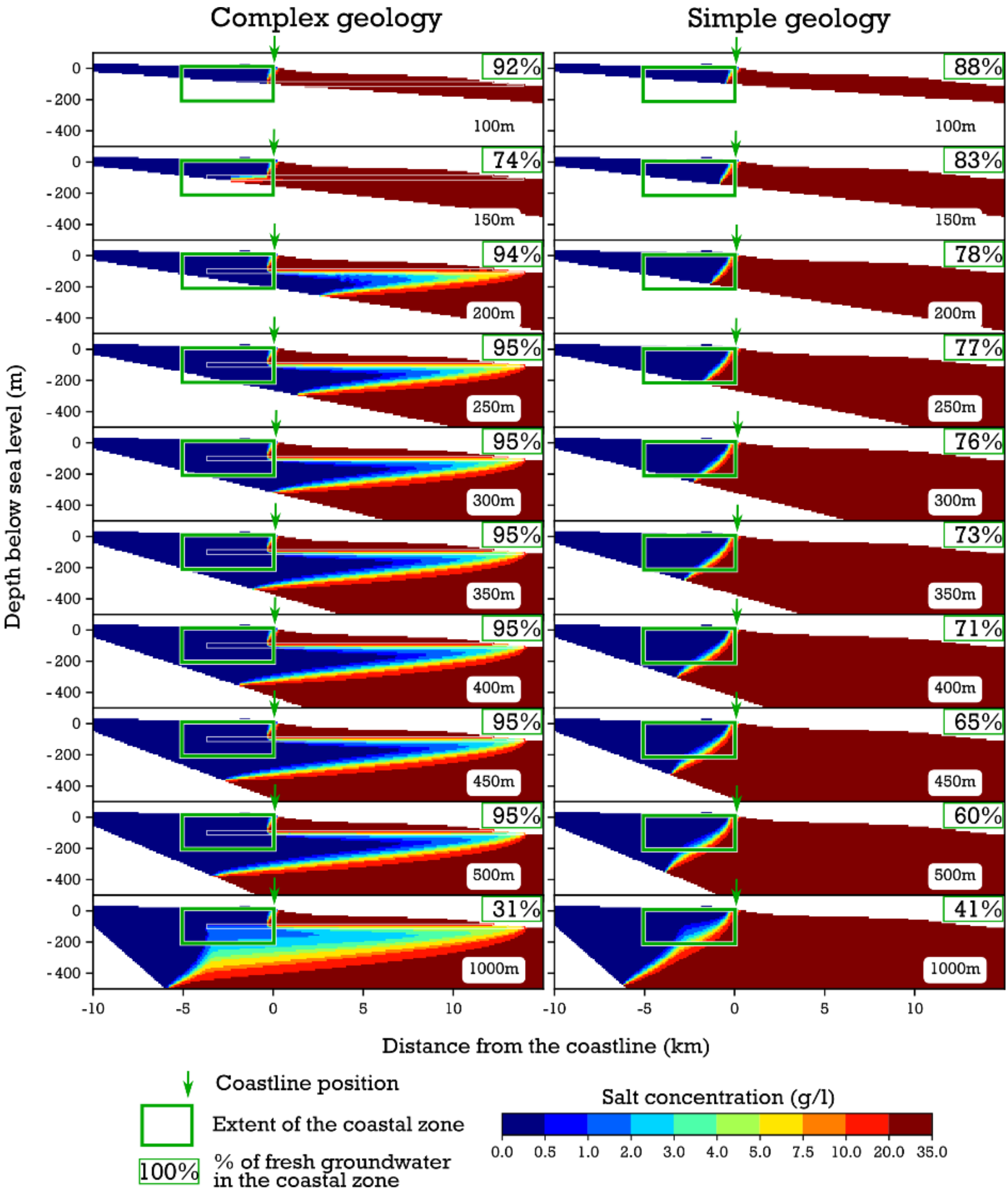

Figure S5. Simulation results for the cross-section located in the Mediterranean coastal plain aquifer, Israel. Salt concentration profiles are given for various sediment thicknesses at the coastline and two different geological scenarios (homogeneous and heterogeneous based on information provided by literature).

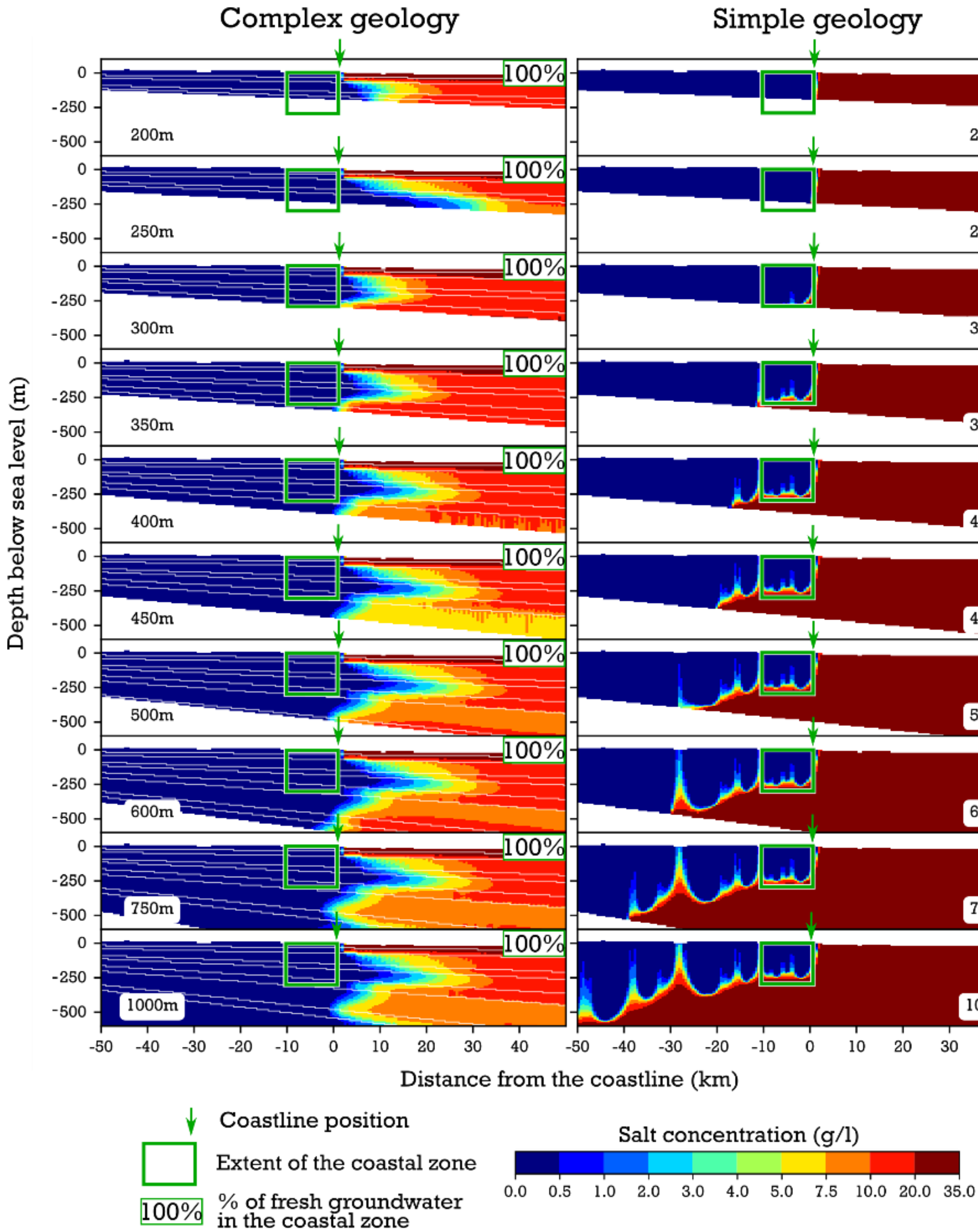

Figure S6. Simulation results for the cross-section located in North Atlantic Coastal Plain, Virginia, USA. Salt concentration profiles are given for various sediment thicknesses at the coastline and two different geological scenarios (homogeneous and heterogeneous based on information provided by literature).